Mixed finite element methods for the Navier–Stokes–Biot model

Sergio Caucao[1,2], Aashi Dalal[3], Tongtong Li[4], and Ivan Yotov[3]

[1] Departamento de Matemática y Física Aplicadas, Universidad Católica de la Santísima Concepción, Concepción, Chile
[2] Grupo de Investigación en Análisis Numérico y Cálculo Científico, GIANuC[2], Chile
scaucao@ucsc.cl
[3] Department of Mathematics, University of Pittsburgh, Pittsburgh, USA
aad100@pitt.edu, yotov@math.pitt.edu
[4] Department of Mathematics, Dartmouth College, Hanover, USA
tongtong.li@dartmouth.edu

Abstract. We present two mixed finite element methods for the quasistatic Navier–Stokes–Biot model. The methods are based on a fully-mixed formulation, using pseudostress, velocity, and vorticity for Navier–Stokes, stress, displacement, and rotation for elasticity, and velocity and pressure for Darcy flow. To handle the advective term, augmenting Galerkin-type terms are introduced in the Navier–Stokes model in the first method, while the second method uses a Banach space formulation. We discuss the relative advantages and disadvantages of the two methods and illustrate their behavior with numerical experiments.

Keywords: Navier–Stokes–Biot · Mixed finite elements · Banach space · Augmented formulation.

1 Introduction

Fluid-poroelastic structure interaction (FPSI) refers to the interaction between a free viscous fluid and the flow in adjacent poroelastic medium. Such physical phenomenon occurs in a wide range of applications, including flows in fractured poroelastic media, surface–subsurface hydrological systems, and cardiovascular flows. The free fluid flow is modeled by the Stokes or the Navier–Stokes equations, while the flow in the poroelastic medium is modeled by the Biot system of poroelasticity. The two regions are coupled through dynamic and kinematic interface conditions, including continuity of normal velocity, balance of fluid force, conservation of momentum, and the Beavers–Joseph–Saffman slip with friction condition. Most of the previous theoretical work on the mathematical model and its numerical approximation has been on the Stokes–Biot model, see e.g. [2, 5, 7, 8, 12, 14, 16, 17, 20]. The Navier–Stokes–Biot model is better suitable for fast flows, such as blood flows or flows through industrial filters. This is a more challenging problem, due to the presence of the nonlinear advective term in the fluid momentum equation. The well-posedness of the model with a non-mixed Darcy formulation is established in [13]. Computational results for the

Navier–Stokes–Biot model can be found in [3, 6, 7, 11]. Recently, an augmented fully-mixed formulation and its mixed finite element approximation have been developed and analyzed in [15].

In this paper we present two mixed finite element methods for the quasistatic Navier–Stokes–Biot model, which are based on a fully-mixed formulation. The Navier–Stokes equations are reformulated in terms of three variables: weakly symmetric nonlinear pseudostress, velocity, and vorticity. The elasticity formulation involves weakly symmetric poroelastic stress, displacement, and rotation, while Darcy flow is modeled by the classical dual mixed velocity-pressure formulation. The weak stress symmetry allows for the use of simpler finite elements. The two methods we consider use the same mixed finite element method for Biot, but differ in the Navier–Stokes discretization. In particular, they differ in the handling of the nonlinear advective term in the Navier–Stokes momentum equation and the related regularity of the fluid velocity. The first method is the augmented method from [15], where redundant Galerkin-type terms arising from the equilibrium and constitutive equations are introduced. As a result, the pseudostress is in H(div) and the fluid velocity is in H^1. The second method is related to the one introduced in [11]. It is based on a Banach space formulation where the divergence of the pseudostress is in $\mathrm{L}^{4/3}$ and the fluid velocity is in L^4. While the augmented method is analyzed in [15], the Banach space method has not been analyzed. We present both semidiscrete methods as degenerate evolution problems in a mixed form, indicating how the techniques from [15] can be applied for the analysis of the Banach space method. We further discuss important features of the two methods, including local mass and momentum conservation, accurate approximations for the stresses and the Darcy velocity, locking-free behavior, and robustness with respect to the physical parameters. We further discuss the relative advantages and disadvantages of the two methods and illustrate their behavior with numerical experiments.

We end this section with some definitions and notation. For a domain $\mathcal{O} \subseteq \mathrm{R}^n$, $n \in \{2, 3\}$, and $p \in [1, +\infty]$, we denote by $\mathrm{L}^p(\mathcal{O})$ and $\mathrm{W}^{s,p}(\mathcal{O})$ the usual Lebesgue and Sobolev spaces. If $p = 2$ we write $\mathrm{H}^s(\mathcal{O})$ in place of $\mathrm{W}^{s,2}(\mathcal{O})$. Let $(\cdot,\cdot)_{\mathcal{O}}$ be the $\mathrm{L}^2(\mathcal{O})$-inner product. For $\Gamma \subset \partial\mathcal{O}$, let $\langle\cdot,\cdot\rangle_{\Gamma}$ be the $\mathrm{L}^2(\Gamma)$ inner product or duality pairing. By $\mathbf{M}$ and $\mathbb{M}$ we will denote the vectorial and tensorial counterparts of the generic scalar functional space M. For vector fields $\mathbf{v} = (v_i)_{i=1:n}$ and $\mathbf{w} = (w_i)_{i=1:n}$, we set the gradient, divergence, and tensor-product operators, as $\nabla\mathbf{v} := \left(\frac{\partial v_i}{\partial x_j}\right)_{i,j=1:n}$, $\mathrm{div}(\mathbf{v}) := \sum_{j=1}^n \frac{\partial v_j}{\partial x_j}$, and $\mathbf{v} \otimes \mathbf{w} := (v_i w_j)_{i,j=1:n}$. For any tensor field $\boldsymbol{\tau} := (\tau_{ij})_{i,j=1:n}$, its deviatoric part is defined as $\boldsymbol{\tau}^{\mathrm{d}} := \boldsymbol{\tau} - \frac{1}{n}\,\mathrm{tr}(\boldsymbol{\tau})\,\mathbf{I}$, where $\mathbf{I}$ is the identity matrix in $\mathrm{R}^{n\times n}$ and $\mathrm{tr}(\boldsymbol{\tau}) := \sum_i^n \tau_{ii}$. We also recall the space $\mathbf{H}(\mathrm{div};\mathcal{O}) := \left\{\mathbf{w} \in \mathbf{L}^2(\mathcal{O}) :\ \mathrm{div}(\mathbf{w}) \in \mathrm{L}^2(\mathcal{O})\right\}$. The space of matrix valued functions with rows in $\mathbf{H}(\mathrm{div};\mathcal{O})$ is denoted by $\mathbb{H}(\mathbf{div};\mathcal{O})$.

2 Model problem

Let $\Omega \subset \mathrm{R}^n$, $n \in \{2, 3\}$ be a Lipschitz domain with polytopal boundary, which is subdivided into two non-overlapping and possibly non-connected regions: a

fluid region Ω_f and a poroelastic region Ω_p. Let $\Gamma_{fp} = \partial\Omega_f \cap \partial\Omega_p$ denote the (nonempty) interface between these regions and let $\Gamma_f = \partial\Omega_f \setminus \Gamma_{fp}$ and $\Gamma_p = \partial\Omega_p \setminus \Gamma_{fp}$ denote the external parts of the boundary $\partial\Omega$. We denote by $\mathbf{n}_f$ and $\mathbf{n}_p$ the unit normal vectors which point outward from $\partial\Omega_f$ and $\partial\Omega_p$, respectively, noting that $\mathbf{n}_f = -\mathbf{n}_p$ on Γ_{fp}. Let $(\mathbf{u}_\star, p_\star)$ be the velocity-pressure pair in $\Omega_\star$ with $\star \in \{f, p\}$, and let $\boldsymbol{\eta}_p$ be the displacement in Ω_p. Let $\mu > 0$ be the fluid viscosity, let ρ be the density, let $\mathbf{f}_\star$ be the body force terms, which do not depend on time, and let q_p be external source or sink term. The flow in Ω_f is governed by the Navier–Stokes equations:

$$\rho\,(\nabla\mathbf{u}_f)\,\mathbf{u}_f - \mathbf{div}(\boldsymbol{\sigma}_f) = \mathbf{f}_f, \quad \mathrm{div}(\mathbf{u}_f) = 0 \ \text{ in } \ \Omega_f \times (0,T], \tag{1a}$$

$$(\boldsymbol{\sigma}_f - \rho\,(\mathbf{u}_f \otimes \mathbf{u}_f))\,\mathbf{n}_f = \mathbf{0} \ \text{ on } \ \Gamma_f^{\mathrm{N}} \times (0,T], \quad \mathbf{u}_f = \mathbf{0} \ \text{ on } \ \Gamma_f^{\mathrm{D}} \times (0,T], \tag{1b}$$

where $\boldsymbol{\sigma}_f := -p_f\,\mathbf{I} + 2\,\mu\,\mathbf{e}(\mathbf{u}_f)$ denotes the stress tensor, $\mathbf{e}(\mathbf{v}) := \dfrac{1}{2}(\nabla\mathbf{v} + (\nabla\mathbf{v})^{\mathrm{t}})$, and $\Gamma_f = \Gamma_f^{\mathrm{N}} \cup \Gamma_f^{\mathrm{D}}$. While the standard Navier–Stokes equations are presented above to describe the behavior of the fluid in Ω_f, in this work we make use of an equivalent version of (1) based on the introduction of a pseudostress tensor combining the stress tensor $\boldsymbol{\sigma}_f$ with the convective term. More precisely, analogously to [10] and [9], we introduce the nonlinear-pseudostress tensor

$$\mathbf{T}_f := \boldsymbol{\sigma}_f - \rho\,(\mathbf{u}_f \otimes \mathbf{u}_f) = -\,p_f\,\mathbf{I} + 2\,\mu\,\mathbf{e}(\mathbf{u}_f) - \rho\,(\mathbf{u}_f \otimes \mathbf{u}_f) \ \text{ in } \ \Omega_f \times (0,T]\,. \tag{2}$$

In this way, applying the matrix trace to the tensor $\mathbf{T}_f$, and utilizing the incompressibility condition $\mathrm{div}(\mathbf{u}_f) = 0$ in $\Omega_f \times (0,T]$, one arrives at

$$p_f = -\frac{1}{n}\,\left(\mathrm{tr}(\mathbf{T}_f) + \rho\,\mathrm{tr}(\mathbf{u}_f \otimes \mathbf{u}_f)\right) \ \text{ in } \ \Omega_f \times (0,T]\,. \tag{3}$$

Hence, replacing back (3) into (2), and using the definition of the deviatoric operator, we obtain $\mathbf{T}_f^{\mathrm{d}} = 2\,\mu\,\mathbf{e}(\mathbf{u}_f) - \rho\,(\mathbf{u}_f \otimes \mathbf{u}_f)^{\mathrm{d}}$. Therefore (1) can be rewritten, equivalently, as the set of equations with unknowns $\mathbf{T}_f$ and $\mathbf{u}_f$, given by

$$\frac{1}{2\,\mu}\,\mathbf{T}_f^{\mathrm{d}} = \nabla\mathbf{u}_f - \boldsymbol{\gamma}_f(\mathbf{u}_f) - \frac{\rho}{2\,\mu}\,(\mathbf{u}_f \otimes \mathbf{u}_f)^{\mathrm{d}} \ \text{ in } \ \Omega_f \times (0,T]\,, \tag{4a}$$

$$-\,\mathbf{div}(\mathbf{T}_f) = \mathbf{f}_f, \quad \mathbf{T}_f = \mathbf{T}_f^{\mathrm{t}} \ \text{ in } \ \Omega_f \times (0,T]\,, \tag{4b}$$

$$\mathbf{T}_f\mathbf{n}_f = \mathbf{0} \ \text{ on } \ \Gamma_f^{\mathrm{N}} \times (0,T], \quad \mathbf{u}_f = \mathbf{0} \ \text{ on } \ \Gamma_f^{\mathrm{D}} \times (0,T]\,, \tag{4c}$$

where $\boldsymbol{\gamma}_f(\mathbf{u}_f) := \dfrac{1}{2}\left(\nabla\mathbf{u}_f - (\nabla\mathbf{u}_f)^{\mathrm{t}}\right)$ is the vorticity. Notice that, as suggested by (3), p_f is eliminated from the present formulation and can be computed afterwards in terms of $\mathbf{T}_f$ and $\mathbf{u}_f$. In addition, the fluid stress $\boldsymbol{\sigma}_f$ can be recovered from (2).

In turn, let $\boldsymbol{\sigma}_e$ and $\boldsymbol{\sigma}_p$ be the elastic and poroelastic stress tensors, respectively:

$$A(\boldsymbol{\sigma}_e) = \mathbf{e}(\boldsymbol{\eta}_p) \ \text{ and } \ \boldsymbol{\sigma}_p := \boldsymbol{\sigma}_e - \alpha_p\,p_p\,\mathbf{I} \ \text{ in } \ \Omega_p \times (0,T]\,, \tag{5}$$

where $0 < \alpha_p \leq 1$ is the Biot–Willis constant, and A is the symmetric and positive definite compliance tensor, satisfying, for some $0 < a_{\min} \leq a_{\max} < \infty$,

$$\forall\, \boldsymbol{\tau} \in \mathrm{R}^{n\times n}, \quad a_{\min}\, \boldsymbol{\tau} : \boldsymbol{\tau} \,\leq\, A(\boldsymbol{\tau}) : \boldsymbol{\tau} \,\leq\, a_{\max}\, \boldsymbol{\tau} : \boldsymbol{\tau} \quad \forall\, \mathbf{x} \in \Omega_p.$$

In the isotropic case A has the form, for all symmetric tensors $\boldsymbol{\tau}$,

$$A(\boldsymbol{\tau}) := \frac{1}{2\mu_p}\left(\boldsymbol{\tau} - \frac{\lambda_p}{2\mu_p + n\lambda_p}\mathrm{tr}(\boldsymbol{\tau})\mathbf{I}\right), \text{ with } A^{-1}(\boldsymbol{\tau}) = 2\mu_p\boldsymbol{\tau} + \lambda_p \mathrm{tr}(\boldsymbol{\tau})\mathbf{I},$$

where $0 < \lambda_{\min} \leq \lambda_p(\mathbf{x}) \leq \lambda_{\max}$ and $0 < \mu_{\min} \leq \mu_p(\mathbf{x}) \leq \mu_{\max}$ are the Lamé parameters. In this case, $\boldsymbol{\sigma}_e := \lambda_p \mathrm{div}(\boldsymbol{\eta}_p)\mathbf{I} + 2\mu_p \mathbf{e}(\boldsymbol{\eta}_p)$, $a_{\min} = \dfrac{1}{2\mu_{\max} + n\lambda_{\max}}$, and $a_{\max} = \dfrac{1}{2\mu_{\min}}$. The poroelasticity region Ω_p is governed by the quasistatic Biot system [4]:

$$-\,\mathbf{div}(\boldsymbol{\sigma}_p) = \mathbf{f}_p, \quad \mu\,\mathbf{K}^{-1}\,\mathbf{u}_p + \nabla\, p_p = \mathbf{0} \ \text{ in } \ \Omega_p \times (0,T], \tag{6a}$$

$$\partial_t\left(s_0\, p_p + \alpha_p\, \mathrm{div}(\boldsymbol{\eta}_p)\right) + \mathrm{div}(\mathbf{u}_p) = q_p \ \text{ in } \ \Omega_p \times (0,T], \tag{6b}$$

$$\mathbf{u}_p \cdot \mathbf{n}_p = 0 \ \text{ on } \ \Gamma_p^{\mathrm{N}} \times (0,T], \quad p_p = 0 \ \text{ on } \ \Gamma_p^{\mathrm{D}} \times (0,T], \tag{6c}$$

$$\boldsymbol{\sigma}_p \mathbf{n}_p = \mathbf{0} \ \text{ on } \ \tilde{\Gamma}_p^{\mathrm{N}} \times (0,T], \quad \boldsymbol{\eta}_p = \mathbf{0} \ \text{ on } \ \tilde{\Gamma}_p^{\mathrm{D}} \times (0,T], \tag{6d}$$

where $\Gamma_p = \Gamma_p^{\mathrm{N}} \cup \Gamma_p^{\mathrm{D}} = \tilde{\Gamma}_p^{\mathrm{N}} \cup \tilde{\Gamma}_p^{\mathrm{D}}$, $0 < s_{0,\min} \leq s_0 \leq s_{0,\max}$ is a constant storage coefficient and $\mathbf{K}$ the symmetric and uniformly positive definite rock permeability tensor, satisfying, for some constants $0 < k_{\min} \leq k_{\max}$,

$$\forall\, \mathbf{w} \in \mathrm{R}^n \quad k_{\min}\, \mathbf{w} \cdot \mathbf{w} \leq (\mathbf{K}\mathbf{w}) \cdot \mathbf{w} \leq k_{\max}\, \mathbf{w} \cdot \mathbf{w} \quad \forall\, \mathbf{x} \in \Omega_p.$$

Next, we introduce the transmission conditions on the interface Γ_{fp}:

$$\mathbf{u}_f \cdot \mathbf{n}_f + \left(\partial_t \boldsymbol{\eta}_p + \mathbf{u}_p\right) \cdot \mathbf{n}_p = 0, \quad \boldsymbol{\sigma}_f \mathbf{n}_f + \boldsymbol{\sigma}_p \mathbf{n}_p = \mathbf{0} \ \text{ on } \ \Gamma_{fp} \times (0,T], \tag{7a}$$

$$\boldsymbol{\sigma}_f \mathbf{n}_f + \mu\, \alpha_{\mathtt{BJS}} \sqrt{\mathbf{K}_{\mathbf{t}}^{-1}}\left((\mathbf{u}_f - \partial_t \boldsymbol{\eta}_p) \cdot \mathbf{t}_f\right)\, \mathbf{t}_f = -\, p_p \mathbf{n}_f \ \text{ on } \ \Gamma_{fp} \times (0,T]. \tag{7b}$$

For simplicity we have adopted notation for a two-dimensional domain in (7b), where $\mathbf{t}_f$ is a unit tangent vector on Γ_{fp}, $\mathbf{K}_{\mathbf{t}} = (\mathbf{K}\,\mathbf{t}_f) \cdot \mathbf{t}_f$, and $\alpha_{\mathtt{BJS}} \geq 0$ is an experimentally determined friction coefficient. The equations in (7a) correspond to mass conservation and conservation of momentum on Γ_{fp}, respectively, whereas (7b) can be decomposed into its normal and tangential components representing the balance of force and the Beavers–Joseph–Saffman (BJS) slip with friction condition, respectively. We observe that the second equations in (7a) and (7b) can be rewritten in terms of tensor $\mathbf{T}_f$ as follows:

$$\mathbf{T}_f \mathbf{n}_f + \rho(\mathbf{u}_f \otimes \mathbf{u}_f)\mathbf{n}_f + \boldsymbol{\sigma}_p \mathbf{n}_p = \mathbf{0}, \tag{8a}$$

$$\mathbf{T}_f \mathbf{n}_f + \rho(\mathbf{u}_f \otimes \mathbf{u}_f)\mathbf{n}_f + \mu\, \alpha_{\mathtt{BJS}} \sqrt{\mathbf{K}_{\mathbf{t}}^{-1}}\left(\left(\mathbf{u}_f - \partial_t \boldsymbol{\eta}_p\right) \cdot \mathbf{t}_f\right) \mathbf{t}_f = -p_p \mathbf{n}_f. \tag{8b}$$

The system of equations (4)–(8) is complemented by the initial condition $p_p(\mathbf{x},0) = p_{p,0}(\mathbf{x})$ in Ω_p, which is used to construct suitable compatible initial data for the rest of the variables in a way that all equations in the system, except for the unsteady conservation of mass equation in (6b), hold at $t = 0$.

3 Weak formulations

In this section we present two mixed variational formulations associated to the coupled problem (4)–(8).

3.1 Augmented mixed formulation

First, we follow an augmented approach developed in [15]. More precisely, we introduce the Hilbert spaces associated to the Navier–Stokes unknowns

$$\begin{aligned}\mathbb{X}_f &:= \Big\{\mathbf{R}_f \in \mathbb{H}(\mathbf{div};\Omega_f) : \quad \mathbf{R}_f\mathbf{n}_f = \mathbf{0} \text{ on } \Gamma_f^{\mathrm{N}}\Big\},\\ \mathbf{V}_f &:= \Big\{\mathbf{v}_f \in \mathbf{H}^1(\Omega_f) : \quad \mathbf{v}_f = \mathbf{0} \text{ on } \Gamma_f^{\mathrm{D}}\Big\}.\end{aligned} \tag{9}$$

In turn, in order to deal with the unknowns in the Biot region we introduce the Hilbert spaces:

$$\begin{aligned}&\mathbb{X}_p := \Big\{\boldsymbol{\tau}_p \in \mathbb{H}(\mathbf{div};\Omega_p) : \quad \boldsymbol{\tau}_p\mathbf{n}_p = \mathbf{0} \text{ on } \tilde{\Gamma}_p^{\mathrm{N}}\Big\},\\ &\mathbf{V}_s := \mathbf{L}^2(\Omega_p), \quad \mathbb{Q}_p := \Big\{\boldsymbol{\chi}_p \in \mathbb{L}^2(\Omega_p) : \quad \boldsymbol{\chi}_p^{\mathrm{t}} = -\boldsymbol{\chi}_p\Big\},\\ &\mathbf{V}_p := \Big\{\mathbf{v}_p \in \mathbf{H}(\mathrm{div};\Omega_p) : \quad \mathbf{v}_p\cdot\mathbf{n} = 0 \text{ on } \Gamma_p^{\mathrm{N}}\Big\}, \quad \mathrm{W}_p := \mathrm{L}^2(\Omega_p).\end{aligned} \tag{10}$$

Next, consider the spaces of traces $\Lambda_p := \mathrm{H}^{1/2}(\Gamma_{fp})$ and $\boldsymbol{\Lambda}_s := [\mathrm{H}^{1/2}(\Gamma_{fp})]^n$. Inspired by [1], we include the structure velocity $\mathbf{u}_s := \partial_t\,\boldsymbol{\eta}_p \in \mathbf{V}_s$ and the Lagrange multipliers $\boldsymbol{\theta} := \mathbf{u}_s|_{\Gamma_{fp}} \in \boldsymbol{\Lambda}_s$ and $\lambda := p_p|_{\Gamma_{fp}} \in \Lambda_p$ as additional unknowns. In addition, we employ a mixed elasticity formulation with weak stress symmetry, introducing as a new unknown the structure rotation operator $\boldsymbol{\gamma}_p := \dfrac{1}{2}\,(\nabla\mathbf{u}_s - (\nabla\mathbf{u}_s)^{\mathrm{t}}) \in \mathbb{Q}_p$. In turn, from the definition of the elastic and poroelastic stress tensors $\boldsymbol{\sigma}_e, \boldsymbol{\sigma}_p$, see (5), we deduce the identities

$$\mathrm{div}(\boldsymbol{\eta}_p) \;=\; A(\alpha_p\,p_p\,\mathbf{I}) : \mathbf{I} + A(\boldsymbol{\sigma}_p) : \mathbf{I} \tag{11}$$

$$\text{and} \quad \partial_t\,A(\boldsymbol{\sigma}_p) \;=\; \nabla\,\mathbf{u}_s - \boldsymbol{\gamma}_p - \partial_t\,A\,(\alpha_p\,p_p\,\mathbf{I}). \tag{12}$$

We group spaces, unknowns and test functions as follows:

$$\begin{aligned}&\mathbf{Q} := \mathbb{X}_p \times \mathrm{W}_p \times \mathbf{V}_p \times \mathbb{X}_f \times \mathbf{V}_f \times \boldsymbol{\Lambda}_s, \quad \mathbf{S} := \Lambda_p \times \mathbf{V}_s \times \mathbb{Q}_p\,,\\ &\mathbf{p} := (\boldsymbol{\sigma}_p, p_p, \mathbf{u}_p, \mathbf{T}_f, \mathbf{u}_f, \boldsymbol{\theta}) \in \mathbf{Q}, \quad \mathbf{r} := (\lambda, \mathbf{u}_s, \boldsymbol{\gamma}_p) \in \mathbf{S}\,,\\ &\mathbf{q} := (\boldsymbol{\tau}_p, w_p, \mathbf{v}_p, \mathbf{R}_f, \mathbf{v}_f, \boldsymbol{\phi}) \in \mathbf{Q}, \quad \mathbf{s} := (\xi, \mathbf{v}_s, \boldsymbol{\chi}_p) \in \mathbf{S}\,.\end{aligned}$$

We test the first equation of (4a), the second equation of (6a), and (12) with arbitrary $\mathbf{R}_f \in \mathbb{X}_f, \mathbf{v}_p \in \mathbf{V}_p$, and $\boldsymbol{\tau}_p \in \mathbb{X}_p$, integrate by parts, and utilize the fact that $\mathbf{T}_f^{\mathrm{d}} : \mathbf{R}_f = \mathbf{T}_f^{\mathrm{d}} : \mathbf{R}_f^{\mathrm{d}}$. We further test (6b) with $w_p \in \mathrm{W}_p$ employing (11), and impose the remaining equations weakly, as well as the symmetry of $\mathbf{T}_f, \boldsymbol{\sigma}_p$, and the transmission conditions in the first equation of (7a) and (8). Then, we can write the augmented weak formulation associated to (4)–(8) in an operator notation as a degenerate evolution problem in a mixed form (see [15, Section 3] for details): Given $\mathbf{f}_f \in \mathbf{L}^2(\Omega_f)$, $\mathbf{f}_p \in \mathbf{L}^2(\Omega_p)$, and $q_p : [0,T] \to \mathrm{L}^2(\Omega_p)$, find $(\mathbf{p}, \mathbf{r}) : [0,T] \to \mathbf{Q} \times \mathbf{S}$ such that, for a.e. $t \in (0,T)$,

$$\begin{aligned} &\partial_t \, \mathcal{E}(\mathbf{p}(t)) + (\mathcal{A} + \mathcal{K}_{\mathbf{u}_f(t)})(\mathbf{p}(t)) + \mathcal{B}'(\mathbf{r}(t)) = \mathcal{F}(t) \quad \text{in } \mathbf{Q}', \\ &-\mathcal{B}(\mathbf{p}(t)) \qquad\qquad\qquad\qquad\qquad\quad = \mathcal{G} \qquad \text{in } \mathbf{S}', \end{aligned} \tag{13}$$

where, given $\mathbf{w}_f \in \mathbf{V}_f$, the operators $\mathcal{A} : \mathbf{Q} \to \mathbf{Q}'$, $\mathcal{K}_{\mathbf{w}_f} : \mathbf{Q} \to \mathbf{Q}'$, and $\mathcal{B} : \mathbf{Q} \to \mathbf{S}'$, are defined by

$$\begin{aligned} \mathcal{A}(\mathbf{p})(\mathbf{q}) &:= \mu \, (\mathbf{K}^{-1}\mathbf{u}_p, \mathbf{v}_p)_{\Omega_p} + \frac{1}{2\,\mu} \, (\mathbf{T}_f^{\mathrm{d}}, \mathbf{R}_f^{\mathrm{d}})_{\Omega_f} + \kappa_1 \, (\mathbf{div}(\mathbf{T}_f), \mathbf{div}(\mathbf{R}_f))_{\Omega_f} \\ &+ \kappa_2 \left(\mathbf{e}(\mathbf{u}_f) - \frac{1}{2\,\mu} \mathbf{T}_f^{\mathrm{d}}, \mathbf{e}(\mathbf{v}_f) \right)_{\Omega_f} + (\mathbf{u}_f, \mathbf{div}(\mathbf{R}_f))_{\Omega_f} - (\mathbf{v}_f, \mathbf{div}(\mathbf{T}_f))_{\Omega_f} \\ &+ (\boldsymbol{\gamma}_f(\mathbf{u}_f), \mathbf{R}_f)_{\Omega_f} - (\mathbf{T}_f, \boldsymbol{\gamma}_f(\mathbf{v}_f))_{\Omega_f} + \langle \mathbf{T}_f \mathbf{n}_f, \mathbf{v}_f \rangle_{\Gamma_{fp}} - \langle \mathbf{R}_f \mathbf{n}_f, \mathbf{u}_f \rangle_{\Gamma_{fp}} \\ &+ \mu \, \alpha_{\mathtt{BJS}} \left\langle \sqrt{\mathbf{K}_{\mathbf{t}}^{-1}} (\mathbf{u}_f - \boldsymbol{\theta}) \cdot \mathbf{t}_f, (\mathbf{v}_f - \boldsymbol{\phi}) \cdot \mathbf{t}_f \right\rangle_{\Gamma_{fp}} \\ &- (p_p, \mathrm{div}(\mathbf{v}_p))_{\Omega_p} + (w_p, \mathrm{div}(\mathbf{u}_p))_{\Omega_p} + \langle \boldsymbol{\sigma}_p \mathbf{n}_p, \boldsymbol{\phi} \rangle_{\Gamma_{fp}} - \langle \boldsymbol{\tau}_p \mathbf{n}_p, \boldsymbol{\theta} \rangle_{\Gamma_{fp}}, \end{aligned} \tag{14}$$

$$\mathcal{K}_{\mathbf{w}_f}(\mathbf{p})(\mathbf{q}) := \frac{\rho}{2\,\mu} ((\mathbf{u}_f \otimes \mathbf{w}_f)^{\mathrm{d}}, \mathbf{R}_f - \kappa_2 \, \mathbf{e}(\mathbf{v}_f))_{\Omega_f} + \rho \, \langle \mathbf{w}_f \cdot \mathbf{n}_f, \mathbf{u}_f \cdot \mathbf{v}_f \rangle_{\Gamma_{fp}},$$

with $\kappa_1, \kappa_2 > 0$ defined in [15, Lemma 3.3] (see also [15, Remark 3.4]), and

$$\mathcal{B}(\mathbf{q})(\mathbf{s}) := (\mathbf{v}_s, \mathbf{div}(\boldsymbol{\tau}_p))_{\Omega_p} + (\boldsymbol{\chi}_p, \boldsymbol{\tau}_p)_{\Omega_p} + \langle \mathbf{v}_f \cdot \mathbf{n}_f + (\boldsymbol{\phi} + \mathbf{v}_p) \cdot \mathbf{n}_p, \xi \rangle_{\Gamma_{fp}},$$

whereas the operator $\mathcal{E} : \mathbf{Q} \to \mathbf{Q}'$ is given by

$$\mathcal{E}(\mathbf{p})(\mathbf{q}) := s_0(p_p, w_p)_{\Omega_p} + (A(\boldsymbol{\sigma}_p + \alpha_p p_p \mathbf{I}), \boldsymbol{\tau}_p + \alpha_p w_p \mathbf{I})_{\Omega_p}, \tag{15}$$

and the functionals $\mathcal{F} \in \mathbf{Q}'$, $\mathcal{G} \in \mathbf{S}'$ are defined as

$$\mathcal{F}(\mathbf{q}) := (q_p, w_p)_{\Omega_p} + (\mathbf{f}_f, \mathbf{v}_f - \kappa_1 \, \mathbf{div}(\mathbf{R}_f))_{\Omega_f} \;\text{ and }\; \mathcal{G}(\mathbf{s}) := (\mathbf{f}_p, \mathbf{v}_s)_{\Omega_p}.$$

The κ_1 and κ_2 terms are redundant consistent Galerkin-type terms arising from the equilibrium and constitutive equations, respectively. Notice that the symmetry of the tensor $\mathbf{T}_f$ is imposed in an ultra-weak sense (see the seventh and eighth terms in (14) and [15, eq. (3.6)] for details).

3.2 Banach space mixed formulation

Alternatively to (13), we now proceed analogously to [9,11] (see also [1, Section 3]) and derive a Banach space weak formulation to deal with the nonlinear pseudostress tensor. To that end, we introduce the spaces:

$$\widetilde{\mathbb{X}}_f := \Big\{ \mathbf{R}_f \in \mathbb{L}^2(\Omega_f) : \quad \mathbf{div}(\mathbf{R}_f) \in \mathbf{L}^{4/3}(\Omega_f) \text{ and } \mathbf{R}_f \mathbf{n}_f = \mathbf{0} \text{ on } \Gamma_f^{\mathrm{N}} \Big\},$$
$$\widetilde{\mathbf{V}}_f := \mathbf{L}^4(\Omega_f), \quad \mathbb{Q}_f := \Big\{ \boldsymbol{\chi}_f \in \mathbb{L}^2(\Omega_f) : \quad \boldsymbol{\chi}_f^{\mathrm{t}} = -\boldsymbol{\chi}_f \Big\}. \tag{16}$$

Notice that for this formulation the vorticity $\boldsymbol{\gamma}_f := \boldsymbol{\gamma}_f(\mathbf{u}_f) \in \mathbb{Q}_f$ as well as the trace of the velocity on the interface $\boldsymbol{\varphi} := \mathbf{u}_f|_{\Gamma_{fp}} \in \boldsymbol{\Lambda}_f := [\mathrm{H}^{1/2}(\Gamma_{fp})]^n$ are included as additional unknowns. For the Biot unknowns we proceed as in (13).

Now, we group the spaces and test functions as follows:

$$\widetilde{\mathbf{Q}} := \big(\widetilde{\mathbb{X}}_f \times \mathbf{V}_p \times \mathbb{X}_p \times \mathrm{W}_p\big) \times \big(\boldsymbol{\Lambda}_f \times \boldsymbol{\Lambda}_s \times \Lambda_p\big), \quad \widetilde{\mathbf{S}} := \widetilde{\mathbf{V}}_f \times \mathbf{V}_s \times \mathbb{Q}_f \times \mathbb{Q}_p,$$
$$\widetilde{\mathbf{p}} := (\mathbf{p}_1, \mathbf{p}_2) = \big((\mathbf{T}_f, \mathbf{u}_p, \boldsymbol{\sigma}_p, p_p), (\boldsymbol{\varphi}, \boldsymbol{\theta}, \lambda)\big) \in \widetilde{\mathbf{Q}}, \quad \widetilde{\mathbf{r}} := (\mathbf{u}_f, \mathbf{u}_s, \boldsymbol{\gamma}_f, \boldsymbol{\gamma}_p) \in \widetilde{\mathbf{S}},$$
$$\widetilde{\mathbf{q}} := (\mathbf{q}_1, \mathbf{q}_2) = \big((\mathbf{R}_f, \mathbf{v}_p, \boldsymbol{\tau}_p, w_p), (\boldsymbol{\psi}, \boldsymbol{\phi}, \xi)\big) \in \widetilde{\mathbf{Q}}, \quad \widetilde{\mathbf{s}} := (\mathbf{v}_f, \mathbf{v}_s, \boldsymbol{\chi}_f, \boldsymbol{\chi}_p) \in \widetilde{\mathbf{S}}.$$

The Banach spaces-based weak formulation is: Given $\mathbf{f}_f \in \mathbf{L}^2(\Omega_f)$, $\mathbf{f}_p \in \mathbf{L}^2(\Omega_p)$, and $q_p : [0,T] \to \mathrm{L}^2(\Omega_p)$, find $(\widetilde{\mathbf{p}}, \widetilde{\mathbf{r}}) : [0,T] \to \widetilde{\mathbf{Q}} \times \widetilde{\mathbf{S}}$ such that, for a.e. $t \in (0,T)$,

$$\begin{aligned} &\partial_t \widetilde{\mathcal{E}}(\widetilde{\mathbf{p}}(t)) + (\widetilde{\mathcal{A}} + \mathcal{C}_{\boldsymbol{\varphi}(t)})(\widetilde{\mathbf{p}}(t)) + (\widetilde{\mathcal{B}}' + \widetilde{\mathcal{K}}_{\mathbf{u}_f(t)})(\widetilde{\mathbf{r}}(t)) = \widetilde{\mathcal{F}}(t) \quad \text{in } \widetilde{\mathbf{Q}}', \\ &-\widetilde{\mathcal{B}}(\widetilde{\mathbf{p}}(t)) = \widetilde{\mathcal{G}} \qquad \text{in } \widetilde{\mathbf{S}}', \end{aligned} \tag{17}$$

where, the operator $\widetilde{\mathcal{E}} : \widetilde{\mathbf{Q}} \to \widetilde{\mathbf{Q}}'$ has the same formula as the one defined in (15). In addition, given $\boldsymbol{\zeta} \in \boldsymbol{\Lambda}_f$ and $\mathbf{w}_f \in \mathbf{V}_f$, the operators $\widetilde{\mathcal{A}} : \widetilde{\mathbf{Q}} \to \widetilde{\mathbf{Q}}'$, $\mathcal{C}_{\boldsymbol{\zeta}} : \widetilde{\mathbf{Q}} \to \widetilde{\mathbf{Q}}'$, $\widetilde{\mathcal{K}}_{\mathbf{w}_f} : \widetilde{\mathbf{Q}} \to \widetilde{\mathbf{S}}'$, and $\widetilde{\mathcal{B}} : \widetilde{\mathbf{Q}} \to \widetilde{\mathbf{S}}'$, are defined by

$$\widetilde{\mathcal{A}}(\widetilde{\mathbf{p}})(\widetilde{\mathbf{q}}) := \mathbf{a}(\mathbf{p}_1)(\mathbf{q}_1) + \mathbf{b}(\mathbf{p}_2)(\mathbf{q}_1) + \mathbf{b}(\mathbf{q}_2)(\mathbf{p}_1) - \mathbf{c}(\mathbf{p}_2)(\mathbf{q}_2),$$
$$\begin{aligned} \mathbf{a}(\mathbf{p}_1)(\mathbf{q}_1) := &\frac{1}{2\mu}(\mathbf{T}_f^{\mathrm{d}}, \mathbf{R}_f^{\mathrm{d}})_{\Omega_f} + \mu(\mathbf{K}^{-1}\mathbf{u}_p, \mathbf{v}_p)_{\Omega_p} \\ &+ (w_p, \mathrm{div}(\mathbf{u}_p))_{\Omega_p} - (p_p, \mathrm{div}(\mathbf{v}_p))_{\Omega_p}, \end{aligned}$$
$$\mathbf{b}(\mathbf{q}_2)(\mathbf{q}_1) := -\langle \mathbf{R}_f \mathbf{n}_f, \boldsymbol{\psi} \rangle_{\Gamma_{fp}} - \langle \boldsymbol{\tau}_p \mathbf{n}_p, \boldsymbol{\phi} \rangle_{\Gamma_{fp}} + \langle \mathbf{v}_p \cdot \mathbf{n}_p, \xi \rangle_{\Gamma_{fp}},$$
$$\begin{aligned} \mathbf{c}(\mathbf{p}_2)(\mathbf{q}_2) := &\, \mu\, \alpha_{\mathtt{BJS}} \left\langle \sqrt{\mathbf{K}_{\mathbf{t}}^{-1}}(\boldsymbol{\varphi} - \boldsymbol{\theta}) \cdot \mathbf{t}_f, (\boldsymbol{\psi} - \boldsymbol{\phi}) \cdot \mathbf{t}_f \right\rangle_{\Gamma_{fp}} \\ &+ \langle \boldsymbol{\psi} \cdot \mathbf{n}_f, \lambda \rangle_{\Gamma_{fp}} + \langle \boldsymbol{\phi} \cdot \mathbf{n}_p, \lambda \rangle_{\Gamma_{fp}} - \langle \boldsymbol{\varphi} \cdot \mathbf{n}_f, \xi \rangle_{\Gamma_{fp}} - \langle \boldsymbol{\theta} \cdot \mathbf{n}_p, \xi \rangle_{\Gamma_{fp}}, \end{aligned}$$
$$\mathcal{C}_{\boldsymbol{\zeta}}(\widetilde{\mathbf{p}})(\widetilde{\mathbf{q}}) := \rho \langle \boldsymbol{\zeta} \cdot \mathbf{n}_f, \boldsymbol{\varphi} \cdot \boldsymbol{\psi} \rangle_{\Gamma_{fp}},$$
$$\widetilde{\mathcal{K}}_{\mathbf{w}_f}(\widetilde{\mathbf{r}})(\widetilde{\mathbf{q}}) := \frac{\rho}{2\mu}((\mathbf{u}_f \otimes \mathbf{w}_f)^{\mathrm{d}}, \mathbf{R}_f)_{\Omega_f},$$
$$\widetilde{\mathcal{B}}(\widetilde{\mathbf{q}})(\widetilde{\mathbf{s}}) := (\mathbf{v}_f, \mathbf{div}(\mathbf{R}_f))_{\Omega_f} + (\mathbf{v}_s, \mathbf{div}(\boldsymbol{\tau}_p))_{\Omega_p} + (\mathbf{R}_f, \boldsymbol{\chi}_f)_{\Omega_f} + (\boldsymbol{\tau}_p, \boldsymbol{\chi}_p)_{\Omega_p},$$

and the functionals $\widetilde{\mathcal{F}} \in \widetilde{\mathbf{Q}}'$, $\widetilde{\mathcal{G}} \in \widetilde{\mathbf{S}}'$ are defined as

$$\widetilde{\mathcal{F}}(\widetilde{\mathbf{q}}) := (q_p, w_p)_{\Omega_p} \text{ and } \widetilde{\mathcal{G}}(\widetilde{\mathbf{s}}) := (\mathbf{f}_f, \mathbf{v}_f)_{\Omega_f} + (\mathbf{f}_p, \mathbf{v}_s)_{\Omega_p}.$$

4 Numerical Methods

For the space discretization we consider mixed finite element approximations for both weak formulations (13) and (17). Let $\mathcal{T}_h^f$ and $\mathcal{T}_h^p$ be affine finite element partitions of Ω_f and Ω_p, respectively, which may be non-matching along the interface Γ_{fp}. We denote by $\mathbf{BDM}_1$ and $\mathrm{P}_1^{\mathrm{dc}}$ the lowest order Brezzi-Douglas-Marini space and discontinuous piecewise linear polynomials, respectively. Then, for both formulations we consider the discrete spaces $\mathbb{X}_{ph} \times \mathbf{V}_{sh} \times \mathbb{Q}_{ph} = \mathbb{BDM}_1 - \mathbf{P}_0 - \mathbb{P}_0$ for stress-displacement-rotation in elasticity, $\mathbf{V}_{ph} \times \mathrm{W}_{ph} = \mathbf{BDM}_1 - \mathrm{P}_0$ for Darcy velocity-pressure, and $\boldsymbol{\Lambda}_{sh} \times \Lambda_{ph} = \mathbf{P}_1^{\mathrm{dc}} - \mathrm{P}_1^{\mathrm{dc}}$ for the Lagrange multipliers, whereas for the Navier–Stokes unknowns we distinct the approaches:

- **Augmented approach:** $\mathbb{X}_{fh} \times \mathbf{V}_{fh} = \mathbb{BDM}_1 - \mathbf{P}_1$ for the pseudostress and velocity.
- **Banach approach:** $\widetilde{\mathbb{X}}_{fh} \times \widetilde{\mathbf{V}}_{fh} \times \mathbb{Q}_{fh} = \mathbb{BDM}_1 - \mathbf{P}_0 - \mathbb{P}_0$ for the pseudostress, velocity and vorticity, and $\boldsymbol{\Lambda}_{fh} = \mathbf{P}_1^{\mathrm{dc}}$ for the additional Lagrange multiplier.

We note that weak stress symmetry allows for the use of the $\mathbb{BDM}_1$ space to approximate the pseudostress and the poroelastic stress. Higher order spaces may also be used [15], but for simplicity we focus here on the lowest order case. The well-posedness of the discrete version of the augmented formulation (13) considering the above discrete spaces, which makes use of a fixed-point strategy along with the theory of degenerate parabolic systems [19], is established in [15, Theorem 5.6], see also [15, Theorem 5.8] for the error analysis. For the analysis of the Banach space method, one can proceed as in [15], due to the similar structure of (13) and (17) as degenerate evolution problems in a mixed form, but now considering arguments similar to [9]. This is a topic of ongoing research.

Both methods exhibit local momentum conservation for the poroelastic stress, local mass conservation for the Darcy fluid, accurate approximations for the stresses and the Darcy velocity, locking-free behavior, and robustness with respect to the physical parameters. Regarding the comparison between the two approaches we comment that for the augmented formulation neither the vorticity $\boldsymbol{\gamma}_f$ nor the Lagrange multiplier $\boldsymbol{\varphi}$ are included as additional unknowns since $\mathbf{u}_f$ is sought in $\mathbf{H}^1(\Omega_f)$ instead of $\mathbf{L}^4(\Omega_f)$. In addition, it provides smooth approximations for both the pseudostress, in $\mathbb{H}(\mathbf{div}; \Omega_f)$, and the fluid velocity, in $\mathbf{H}^1(\Omega_f)$. On the other hand, the Banach space formulation, although more expensive in terms of number of variables, utilizes the natural spaces arising from the application of the Cauchy–Schwarz and Hölder inequalities to the terms resulting from the testing and integration by parts of the equations of the model. One consequence is that it exhibits local momentum conservation for the pseudostress, due to the $\mathbb{BDM}_1 - \mathbf{P}_0$ pseudostress-velocity pair. Furthermore, it can be implemented as a multipoint stress-flux mixed finite element method, which allows for local elimination of the stresses and the Darcy velocity, as well as the vorticity and rotation in the case of $\mathbb{P}_1$ elements for these two variables [11].

5 Numerical results

We present two numerical experiments to illustrate the convergence and applicability of the methods, using the backward Euler method for time discretization.

Example 1: Convergence test. In this example we study numerically the convergence in space, using unstructured triangular grids. The total simulation time is $T = 0.01$ and the time step is $\Delta t = 10^{-3}$, which is sufficiently small, so that the time discretization error does not affect the convergence rates. The domain consists of $\Omega_f = (0,1) \times (0,1)$, $\Gamma_{fp} = (0,1) \times \{0\}$, and $\Omega_p = (0,1) \times (-1,0)$. We take $\Gamma_f^D = (0,1) \times \{1\}$, $\Gamma_p^D = (0,1) \times \{-1\}$, and $\tilde{\Gamma}_p^D = \Gamma_p$. The true solution in the Navier–Stokes region is

$$\mathbf{u}_f = \exp(t) \begin{pmatrix} \sin(\pi x)\cos(\pi y) \\ -\sin(\pi y)\cos(\pi x) \end{pmatrix}, \quad p_f = \exp(t)\sin(\pi x)\cos\left(\frac{\pi y}{2}\right) + 2\pi\cos(\pi t).$$

The Biot solution is chosen accordingly to satisfy the interface conditions (7):

$$p_p = \exp(t)\sin(\pi x)\cos\left(\frac{\pi y}{2}\right), \quad \mathbf{u}_p = -\frac{1}{\mu}\mathbf{K}\nabla p_p, \quad \boldsymbol{\eta}_p = \sin(\pi t)\begin{pmatrix} \cos(y) - 3x \\ y + 1 \end{pmatrix}.$$

The model parameters are

$$\mu = 1, \quad \rho = 1, \quad \lambda_p = 1, \quad \mu_p = 1, \quad s_0 = 1, \quad \mathbf{K} = \mathbf{I}, \quad \alpha_p = 1, \quad \alpha_{\mathtt{BJS}} = 1.$$

We run a sequence of mesh refinements with non-matching grids along Γ_{fp}. For the sake of space we display the results only for the Banach formulation. Nevertheless, we stress that both schemes (13) and (17) converge optimally, see [15] for convergence studies of the augmented method. The results are reported on Table 1. We note that the fluid pressure and displacement at t_n are recovered by the discrete version of (3) and the formula $\boldsymbol{\eta}_p^n = \Delta t\, \mathbf{u}_s^n + \boldsymbol{\eta}_p^{n-1}$, respectively. We observe at least first order convergence for all subdomain variables in their natural norms. The Lagrange multiplier variables, which are approximated in $\mathbf{P}_1^{\mathrm{dc}} - \mathbf{P}_1^{\mathrm{dc}} - \mathrm{P}_1^{\mathrm{dc}}$, exhibit second order convergence in the L^2-norm on Γ_{fp}, which is consistent with the order of approximation.

Example 2: Air flow through a filter. The setting in this example is similar to the one presented in [18], where the Navier–Stokes–Darcy model is considered. The domain is a two-dimensional rectangular channel with length 2.5m and width 0.25m, which on the bottom center is partially blocked by a square poroelastic filter of length and width 0.2m, see Fig. 1 (top). The model parameters are set as

$$\mu = 1.81 \times 10^{-8}\ \text{kPa s}, \quad \rho = 1.225 \times 10^{-3}\ \text{Mg/m}^3, \quad s_0 = 7 \times 10^{-2}\ \text{kPa}^{-1},$$
$$\mathbf{K} = [0.505, -0.495; -0.495, 0.505] \times 10^{-6}\ \text{m}^2, \quad \alpha_{\mathtt{BJS}} = 1.0, \quad \alpha = 1.0.$$

Note that μ and ρ are parameters for air. The permeability tensor $\mathbf{K}$ is obtained by rotating the identity tensor by a 45° rotation angle in order to consider the effect of material anisotropy on the flow. We further consider a stiff material in

iter	h_f	$\|\mathbf{e}_{\mathbf{T}_f}\|_{\ell^2(0,T;\mathbb{X}_f)}$ error	rate	$\|\mathbf{e}_{\mathbf{u}_f}\|_{\ell^2(0,T;\mathbf{V}_f)}$ error	rate	$\|\mathbf{e}_{\boldsymbol{\gamma}_f}\|_{\ell^2(0,T;\mathbb{Q}_f)}$ error	rate	$\|\mathbf{e}_{p_f}\|_{\ell^2(0,T;\mathrm{L}^2(\Omega_f))}$ error	rate
2.2	0.1964	1.6E-01	–	1.2E-02	–	2.7E-02	–	7.2E-03	–
2.2	0.0997	7.9E-02	1.0059	5.6E-03	1.0686	1.3E-02	1.0960	2.5E-03	1.5343
2.2	0.0487	3.9E-02	1.0028	2.7E-03	1.0358	6.5E-03	0.9605	1.1E-03	1.2087
2.2	0.0250	1.9E-02	1.0323	1.3E-03	1.0249	3.3E-03	1.0319	5.1E-04	1.1042
2.2	0.0136	9.7E-03	1.1425	6.7E-04	1.1440	1.6E-03	1.1575	2.5E-04	1.2087
2.2	0.0072	4.8E-03	1.1040	3.3E-04	1.1152	8.1E-04	1.0939	1.2E-04	1.1099

h_p	$\|\mathbf{e}_{\boldsymbol{\sigma}_p}\|_{\ell^\infty(0,T;\mathbb{X}_p)}$ error	rate	$\|\mathbf{e}_{\mathbf{u}_s}\|_{\ell^2(0,T;\mathbf{V}_s)}$ error	rate	$\|\mathbf{e}_{\boldsymbol{\gamma}_p}\|_{\ell^2(0,T;\mathbb{Q}_p)}$ error	rate	$\|\mathbf{e}_{\mathbf{u}_p}\|_{\ell^2(0,T;\mathbf{V}_p)}$ error	rate	$\|\mathbf{e}_{p_p}\|_{\ell^\infty(0,T;\mathrm{W}_p)}$ error	rate
0.2828	2.7E-01	–	4.3E-02	–	8.6E-02	–	1.0E-01	–	7.5E-02	–
0.1646	1.4E-01	1.2732	2.2E-02	1.2275	2.2E-02	2.5658	5.0E-02	1.3529	3.8E-02	1.2480
0.0779	6.7E-02	0.9650	1.1E-02	0.9618	4.9E-03	1.9684	2.4E-02	0.9896	1.9E-02	0.9328
0.0434	3.4E-02	1.1690	5.4E-03	1.1866	1.5E-03	2.0132	1.2E-02	1.2361	9.4E-03	1.2150
0.0227	1.7E-02	1.0634	2.7E-03	1.0668	5.8E-04	1.4877	5.9E-03	1.0739	4.7E-03	1.0658
0.0124	8.4E-03	1.1462	1.4E-03	1.1456	2.7E-05	1.2917	2.9E-03	1.1452	2.4E-03	1.1429

$\|\mathbf{e}_{\boldsymbol{\eta}_p}\|_{\ell^2(0,T;\mathbf{L}^2(\Omega_p))}$ error	rate	h_{tf}	$\|\mathbf{e}_{\boldsymbol{\varphi}}\|_{\ell^2(0,T;\mathbf{L}^2(\Gamma_{fp}))}$ error	rate	h_{tp}	$\|\mathbf{e}_{\boldsymbol{\theta}}\|_{\ell^2(0,T;\mathbf{L}^2(\Gamma_{fp}))}$ error	rate	$\|\mathbf{e}_{\lambda}\|_{\ell^2(0,T;\mathrm{L}^2(\Gamma_{fp}))}$ error	rate
2.7E-04	–	1/8	6.5E-03	–	1/5	9.3E-03	–	1.1E-03	–
1.4E-04	1.2253	1/16	1.5E-03	2.0936	1/10	2.8E-03	1.7323	2.7E-04	2.0019
6.7E-05	0.9615	1/32	3.7E-04	2.0245	1/20	6.8E-04	2.0386	6.7E-05	1.9977
3.4E-05	1.1865	1/64	9.4E-05	1.9893	1/40	1.7E-04	1.9889	1.7E-05	1.9941
1.7E-05	1.0668	1/128	2.4E-05	1.9613	1/80	4.3E-05	1.9925	4.3E-06	1.9826
8.4E-06	1.1456	1/256	5.6E-06	2.0985	1/160	1.1E-05	2.0094	1.1E-06	1.9632

Table 1. [Example 1] Average number of Newton iterations, mesh sizes, errors, rates of convergences.

the poroelastic region with parameters: $\lambda_p = 1{\times}10^4$kPa and $\mu_p = 1{\times}10^5$kPa. The top and bottom of the domain are rigid, impermeable walls. The flow is driven by a pressure difference $\Delta p = 2 \times 10^{-6}$ kPa between the left and right boundary, see Fig. 1 (bottom) for the boundary conditions. The body force terms $\mathbf{f}_f$ and $\mathbf{f}_p$ and external source q_p are set to zero. For the initial conditions, we consider

$$p_{p,0} = 100 \text{ kPa}, \quad \boldsymbol{\sigma}_{p,0} = -\alpha_p\, p_{p,0}\, \mathbf{I}, \quad \mathbf{u}_{f,0} = \mathbf{0} \text{ m/s}.$$

The computational matching grid along Γ_{fp} has a characteristic parameter $h = \max\{h_f, h_p\} = 0.018$. The total simulation time is $T = 400$s with $\Delta t = 1$s.

For the sake of space we display the results only for the augmented formulation. The computed magnitude of the velocities and pressures are displayed in Figs. 2 and 3, respectively. We observe high velocity in the narrow open channel above the filter. Vortices develop behind the obstacle, which travel with the fluid and are smoothed out at later times. A sharp pressure gradient is observed in the region above the filter, as well as within the filter, where the permeability anisotropy affects both the pressure and velocity fields. This example illustrates the ability of the mixed method to produce oscillation-free solution in a regime

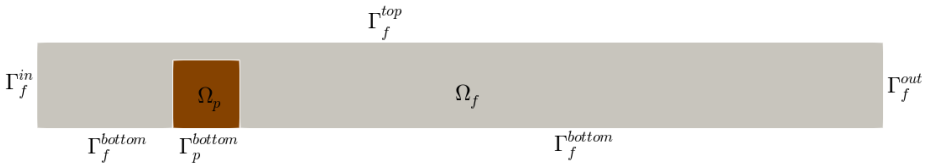

$$\boldsymbol{\sigma}_f \mathbf{n}_f = -p_{in}\mathbf{n}_f \ \text{ on } \ \Gamma_f^{in}, \quad \boldsymbol{\sigma}_f \mathbf{n}_f = -p_{out}\mathbf{n}_f \ \text{ on } \ \Gamma_f^{out}$$
$$p_{in} = p_{ref} + 2 \times 10^{-6}\text{kPa}, \quad p_{out} = p_{ref}, \quad \mathbf{u}_f = 0 \ \text{ on } \ \Gamma_f^{top} \cup \Gamma_f^{bottom}$$
$$\mathbf{u}_s = \mathbf{0} \ \text{ and } \ \mathbf{u}_p \cdot \mathbf{n}_p = 0 \ \text{ on } \ \Gamma_p^{bottom}$$

Fig. 1. [Example 2] Top: computational domain and boundaries; channel Ω_f in gray, filter Ω_p in brown. Bottom: boundary conditions with $p_{ref} = 100\,\text{kPa}$.

of challenging physical parameters, including small viscosity and permeability and large Lamé coefficients.

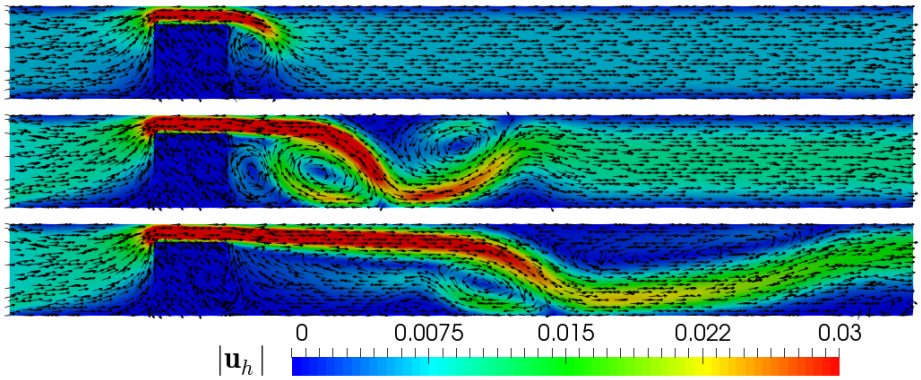

Fig. 2. [Example 2] Computed velocities $\mathbf{u}_{fh}$ and $\mathbf{u}_{ph}$ (arrows not scaled) and their magnitudes at times $t \in \{20, 80, 400\}$ (from top to bottom).

Acknowledgments This work was supported in part by ANID-Chile through the projects Centro de Modelamiento Matemático (FB210005) and Fondecyt 11220393; and by NSF grant DMS 2111129.

References

1. Ambartsumyan, I., Ervin, V.J., Nguyen, T., Yotov, I.: A nonlinear Stokes-Biot model for the interaction of a non-Newtonian fluid with poroelastic media. ESAIM Math. Model. Numer. Anal. **53**(6), 1915–1955 (2019)

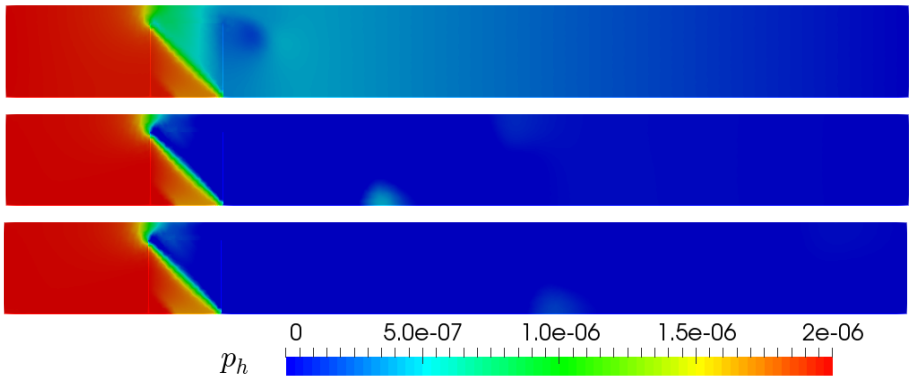

Fig. 3. [Example 2] Computed pressures $p_{fh} - p_{ref}$ and $p_{ph} - p_{ref}$ at times $t \in \{20, 80, 400\}$ (from top to bottom).

2. Ambartsumyan, I., Khattatov, E., Yotov, I., Zunino, P.: A Lagrange multiplier method for a Stokes-Biot fluid-poroelastic structure interaction model. Numer. Math. **140**(2), 513–553 (2018)
3. Badia, S., Quaini, A., Quarteroni, A.: Coupling Biot and Navier-Stokes equations for modelling fluid-poroelastic media interaction. J. Comput. Phys. **228**(21), 7986–8014 (2009)
4. Biot, M.: General theory of three-dimensional consolidation. J. Appl. Phys. **12**, 155–164 (1941)
5. Bociu, L., Canic, S., Muha, B., Webster, J.T.: Multilayered poroelasticity interacting with Stokes flow. SIAM J. Math. Anal. **53**(6), 6243–6279 (2021)
6. Bukač, M.: A loosely-coupled scheme for the interaction between a fluid, elastic structure and poroelastic material. J. Comput. Phys. **313**, 377–399 (2016)
7. Bukač, M., Yotov, I., Zunino, P.: An operator splitting approach for the interaction between a fluid and a multilayered poroelastic structure. Numer. Methods Partial Differential Equations **31**(4), 1054–1100 (2015)
8. Bukač, M., Yotov, I., Zakerzadeh, R., Zunino, P.: Partitioning strategies for the interaction of a fluid with a poroelastic material based on a Nitsche's coupling approach. Comput. Methods Appl. Mech. Eng. **292**, 138–170 (2015)
9. Camaño, J., García, C., Oyarzúa, R.: Analysis of a momentum conservative mixed-FEM for the stationary Navier-Stokes problem. Numer. Methods Partial Differential Equations **37**(5), 2895–2923 (2021)
10. Camaño, J., Gatica, G.N., Oyarzúa, R., Tierra, G.: An augmented mixed finite element method for the Navier-Stokes equations with variable viscosity. SIAM J. Numer. Anal. **54**(2), 1069–1092 (2016)
11. Caucao, S., Li, T., Yotov, I.: A cell-centered finite volume method for the navier–stokes/biot model. In: Klöfkorn, R., Keilegavlen, E., Radu, F.A., Fuhrmann, J. (eds.) Finite Volumes for Complex Applications IX - Methods, Theoretical Aspects, Examples. pp. 325–333. Springer International Publishing, Cham (2020)
12. Caucao, S., Li, T., Yotov, I.: A multipoint stress-flux mixed finite element method for the Stokes-Biot model. Numer. Math. **152**(2), 411–473 (2022)
13. Cesmelioglu, A.: Analysis of the coupled Navier-Stokes/Biot problem. J. Math. Anal. Appl. **456**(2), 970–991 (2017)

14. Cesmelioglu, A., Chidyagwai, P.: Numerical analysis of the coupling of free fluid with a poroelastic material. Numer. Methods Partial Differential Equations **36**(3), 463–494 (2020)
15. Li, T., Caucao, S., Yotov, I.: An augmented fully mixed formulation for the quasistatic Navier–Stokes–Biot model. IMA J. Numer. Anal. p. drad036 (06 2023). https://doi.org/10.1093/imanum/drad036
16. Li, T., Yotov, I.: A mixed elasticity formulation for fluid–poroelastic structure interaction. ESAIM Math. Model. Numer. Anal. **56**(1), 01–40 (2022)
17. Ruiz-Baier, R., Taffetani, M., Westermeyer, H.D., Yotov, I.: The Biot-Stokes coupling using total pressure: formulation, analysis and application to interfacial flow in the eye. Comput. Methods Appl. Mech. Engrg. **389**, Paper No. 114384, 30 (2022)
18. Schneider, M., Weishaupt, K., Gläser, D., Boon, W.M., Helmig, R.: Coupling staggered-grid and MPFA finite volume methods for free flow/porous-medium flow problems. J. Comput. Phys. **401**, 109012, 17 (2020)
19. Showalter, R.E.: Monotone Operators in Banach Space and Nonlinear Partial Differential Equations. Mathematical Surveys and Monographs, 49. American Mathematical Society, Providence, RI (1997)
20. Showalter, R.E.: Poroelastic filtration coupled to Stokes flow. Control theory of partial differential equations. Lect. Notes Pure Appl. Math., 242, Chapman & Hall/CRC, Boca Raton, FL pp. 229–241 (2005)